PCCP

PAPER

Molecular Dynamics Simulations of the Structure and the Morphology of Graphene/Polymer Nanocomposites

Received 00th January 20xx,
Accepted 00th January 20xx

DOI: 10.1039/x0xx00000x

www.rsc.org/

S. Güryel[a], M. Walker[b], P. Geerlings[*a] F. De Proft[a], Mark R. Wilson[b]

The structure and morphology of three polymer/graphene nanocomposites have been studied using classical molecular dynamics (MD) simulations. The simulations use 10-monomer oligomeric chains of three polymers: polyethylene (PE), polystyrene (PS) and polyvinylidene fluoride (PVDF). The structure of the polymer chains at the graphene surface have been investigated and characterized by pair correlation functions (PCF), *g(r), g(ϑ)* and *g(r,ϑ)*. In addition, the influence of the temperature on the graphene/polymer interactions has been analysed for each of the three polymer/graphene nanocomposite systems. The results indicate that graphene induces order in both the PE and PVDF systems by providing a nucleation site for crystallisation, steering the growth of oligomer crystals according to the orientation of the graphene sheet, whereas the PS system remains disordered in the presence of graphene. The overall results are in line with the findings in a recent quantumchemical study by some of the present authors.

Introduction

Graphene consists of a monolayer of carbon atoms neatly packed into a two-dimensional (2D) honeycomb lattice structure. It has recently gained overwhelming attention[1] due to its outstanding mechanical, electrical and thermal properties, making it ideal for miscellaneous practical applications in different fields. Given their multifunctional properties, graphene/polymer composites are extensively utilized as both structural and functional composites in various applications, including electromagnetic interference (EMI), microwave absorption, flexible electronics, supercapacitors, biomedical devices, and many more. Particularly, in view of its remarkable intrinsic properties, graphene can also be considered for use as a nanofiller in polymer composites to reinforce their mechanical and electrical properties. The chemical modification of graphene sheets via organic oligomeric and polymeric chains constitutes an optimal route to enhance the compatibility of these graphene-based nanoparticles with polymeric media.

In graphene research, special attention has been given to understanding the properties of graphene-polymer nanocomposites. Many studies on graphene-polymer composites point to the significant improvement in mechanical, thermal and electrical[2] properties as compared to pure graphene.[3] Das and co-workers[4] have examined the mechanical properties of polyvinyl alcohol (PVA) and polymethyl methacrylate (PMMA) with each polymer functionalized by the inclusion of few-layer graphene (FG). They observed that the elastic modulus and hardness were improved by adding 0.6 wt% of graphene to the pure polymer systems. Additionally, increased crystallinity of PVA has been reported, when graphene is included in a graphene/PVA nanocomposite system.[4]

In support of the experimental findings on graphene-polymer nanocomposites, a molecular-level understanding of the behaviour of these systems using computational models is of high importance. A number of molecular dynamics (MD) simulation studies on graphene-polymer systems have been reported recently. Among them, Rissanou *et al*.[5] investigated the effect of graphene layers on the structural and dynamical properties of three well-known polymers, polyethylene (PE), polystyrene (PS) and poly(methyl methacrylate) (PMMA). They showed that graphene sheets have a great impact on both the structure and dynamics of the polymer chains. They also indicated that PE chains exhibit greater mobility on the surface as compared to PS and PMMA. PE is one of the most important polymer materials due to its versatility (both flexible and rigid forms of PE are possible, dependent on the extent and type of branching and the degree of crystallinity); hence, it is an ideal potential candidate for carbon-based nanocomposites. An MD simulation of a polyethylene/carbon nanotube system by Minoia *et al.*,[6] suggests that the adsorption of PE polymer chains is influenced by changing the diameter of the nanotube

[a] *Research Group General Chemistry (ALGC), Vrije Universiteit Brussel (VUB), Pleinlaan 2, B-1050 Brussels, Belgium. E-mail: pgeerlin@vub.ac.be*
[b] *Department of Chemistry, Durham University, South Road, DH1 3LE, Durham, United Kingdom.*

† Footnotes relating to the title and/or authors should appear here. Electronic Supplementary Information (ESI) available: [details of any supplementary information available should be included here]. See DOI: 10.1039/x0xx00000x

and by the presence of hydroxyl groups on the nanotube surface. A molecular dynamics study on the effect of the functionalisation of graphene and its interaction with polymers[7] has been reported by Lv *et al.*[8] They suggest that the chemical modification of graphene has a significant impact on the interfacial-bonding between the polymer and graphene sheet. Recent Molecular Dynamics studies on functionalized graphene based nano-composites pointed towards the opportunities of functionalized graphene sheets in the design of new, very strong multifunctional materials, achieving better material performance.[9 10]

Polyvinylidene fluoride (PVDF) is one of the most studied polymers due to its high piezoelectric properties. It is known for its polymorphism and complicated microstructure:[11,12] PVDF exhibits at least five well-known crystalline forms, denoted as α and δ, β, γ and ε.[13, 14] Both the α and δ phases display an alternating *trans-gauche* (*TGTG*) conformation. The α form is the most common phase and the thermodynamically most stable polymorph. The β crystal phase with an *all trans* (*TTT*) planar zigzag conformation is important because of its piezoelectric properties. The β crystal phase is obtained by various methods such as mechanical deformation,[15,16] melt crystallization at high pressures[17] and more recently by addition of nanoparticles.[18] The γ and ε structures of PVDF with a T_3GT_3G conformation are not as abundant or as polar as the α and β forms.[19] The relationship between structure and physical properties of thin PVDF/multi-walled carbon nanotube (MWNT) composite films were studied by Hong *et al.*[20] MWNT were used as an internal mixer in PVDF to produce a polar β-form crystal structure of PVDF. Rahman *et al*.[21] have investigated PVDF–graphene nanocomposite films which are prepared by simple solution casting of PVDF/graphene oxide (PVDF/GO) solution. The loading of GO into the nanocomposite system improves the ferroelectric behaviour and dielectric constant compared to those of pure PVDF.

Recently, PM6 and PM6-D3H4X studies (accounting for dispersion correction, hydrogen and halogen bonding) were conducted by some of the present authors to analyse the interaction of PE, PS and PVDF with a graphene sheet, scrutinising the influence of chain conformation. They indicate that the overall interaction strength is strongly influenced by the specific polymer structure and chain conformation, although all these polymers clearly exhibit attractive interactions with the graphene sheet due to dispersion.[22] As seen in this study by some of the present authors a typical two to fourfold increase with broadening of the interaction range is found for the interaction of PE,PS and PVDF when passing from PM6 to the H-bonding and dispersion corrected level :PE from -17.5 to -50.5 , PS : from -6.3 to -26.9 ; PVDF – 20.8 to -50.9 (strongest interacting conformer)(all values in energy per unit area (kcal mol^{-1} /nm^{-2})).In detail, PVDF has three common conformations and among them PVDF-zigzag ("F-up", H atoms oriented towards the graphene surface and F atoms in the opposite direction) has the strongest interaction with the graphene surface. Likewise, it displays the highest binding energy per unit area, making it the most desirable polymer for making nanocomposites. Although PS has a strong interaction with graphene, it covers a much broader area (i.e. the contact area of the single chain on the surface) thus lowering the interaction energy per unit area. In contrast, PE has a rather strong interaction with pristine graphene and an interaction energy per unit area comparable to PVDF. PE and PVDF zigzag ("F-up") have a comparable binding strength due to their similar geometry: in both cases, the H site of the polymers is in a "face-to-face" alignment with the graphene surface. However, in the case of PVDF ("F-up"), graphene directly interacts via the H atoms, yielding a stronger interaction due to the electronegativity of F, which is not present in PE.[22]

In this paper, we provide molecular-level insights into the interactions of different polymers with graphene using a molecular dynamics simulation strategy for polymer/graphene nanocomposites. Our particular emphasis is on the comprehensive analysis of energetic and structural properties. To achieve this, we choose three host polymers: PE, PS and PVDF. The choice of polymers is guided by the ability of the three polymer hosts to demonstrate diverse application possibilities in the case of a graphene/polymer nanocomposite; and because each host demonstrates potentially useful physical properties: for PS, its rigidity and transparency, for PVDF its electronic properties and for PE its flexibility and its chemical resistance.

This paper focuses on a comparison of the behaviour of these three systems with special attention paid to the nature of the intermolecular interactions of the graphene and the accompanying polymer. To this end, the structural aspects of polymer chain on the graphene surface have been characterized by pair correlation functions (PCF). Also, the influence of temperature on graphene/polymer interactions has been analysed for each nanocomposite.

Computational Details

Classical molecular dynamics simulations were performed for each nanocomposite system described below. Simulations were carried out in the constant-*NPT* ensemble, with the mean pressure kept constant at 1 atm, using a Rahman-Parrinello barostat,[23] and the mean temperature fixed at 500 K using a Nosé-Hoover thermostat.[24,25] 50 ns production runs were carried out for each system, following initial equilibration runs. All simulations used the GROMACS 4.6.5 package.[26]

The Optimized Protein Liquid Simulations (OPLS) atomistic force field, was used to describe the intermolecular and intramolecular interactions of the considered polymers.[27,28] OPLS currently represents the best force field for long hydro-carbon polymers, including parametrization for fluorine. [29,30]. The carbon atoms within the graphene are treated as atom types CA, the same as the aromatic carbon atoms in polystyrene. A further differentiation is beyond the scope of this study. Electrostatic interactions were calculated using particle mesh Ewald[31] with a real space cut-off of 11 Å. Lennard-Jones interactions were truncated at 11 Å. Neighbour lists were updated every 15 time steps using a list cut-off radius of 11 Å. Periodic boundary conditions (PBC), using a

simulation box with initial dimensions of 68 x 68 x 68 Å^3, was applied for all systems. Bond constraints were solved using the Linear Constraint Solver (LINCS) algorithm[32] using the fourth lincs order.

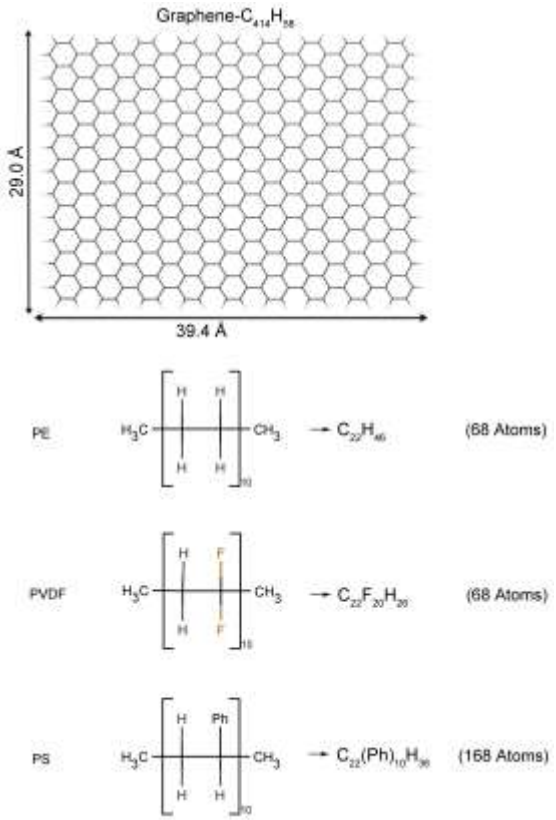

Scheme 1: Schematic representation of the polymers and the graphene sheet considered in this study.

Molecular dynamics simulations of three different polymer-graphene nanocomposites, PE-Graphene, PS-Graphene and PVDF-Graphene (see Scheme 1), were carried out as follows. In all cases, the polymer chains consisted of 10 monomers and each polymer fragment consisted of 22 backbone carbon atoms. A single graphene sheet with a width of 39.4 Å and a length of 29.0 Å was used for the simulations of polymer-graphene composites. In this graphene model the carbon atoms at the edges were capped with 58 hydrogen atoms in order to avoid the unsaturated boundary effect ($C_{414}H_{58}$). The reference bulk systems consisted of 500 10-mer chains for PE and PVDF and 200 10-mer chains for PS. The number of chains was chosen such that each simulation box would retain approximately the same size during the simulation. The simulations were setup by placing 500 relaxed PE and PVDF, or 200 syndiotactic PS chains and the single graphene sheet into a box; giving a total number of atoms of 34472 for PE and PVDF, 34072 for PS. For equilibrating each polymer/graphene system, we followed a procedure in which the systems were first equilibrated at high temperature (800 K) and pressure (200 atm) in relatively short constant-*NPT* runs (100 ps), eliminating any voids in the system. The pressure was then reduced in four short (100 ps) constant-*NPT* simulation runs, in increments of 50 atm, to achieve the target pressure of 1 atm. The detailed pressure and temperature variation was as follows (all time intervals being 0.5 ns): 800K-200atm, 800K-150atm, 800K-100atm, 800K-50atm, 800K-20atm, 800K-10atm, 800K-5atm, 800K-1atm, 700K-1atm, 600K-1atm, 500K-1atm highlighting how extensive the equilibration was. After this pre-equilibration, a lengthy equilibration run (1 ns, using 1 fs time steps) at the target temperature (500 K), we performed a constant-*NPT* production run for 50 ns for each system; these were used for in-depth analyses (using LINCS with a time step of 2 fs).

A temperature of 500 K was chosen on the basis that this is higher than the melting and glass-transition temperatures of the polymers (T_m = 410, 440, 510 K and T_g = 190, 240, 360 K for PE, PVDF, and PS, respectively), although in experimental conditions these temperatures will depend on the chain length or molecular weight of the polymers.

Simulations of the polymer with the graphene flake removed were performed initially as an NPT simulation, using the equilibrated structure of the polymer with the graphene sheet, with a vacuum replacing the graphene. This system was heated to 800K for 5 ns to fully melt the polymer and then cooled to 500K in a single step and equilibrated for 25 ns.

A summary of the non-bonded force field parameters used are depicted in Table 1.

Atom	ε / kJ mol^{-1}	σ / Å
Polymer backbone carbon C3	0.4393	0.375
Polymer backbone hydrogen HC	0.1255	0.250
Polymer Fluorine F	0.2552	0.312
Aromatic carbon CA	0.2929	0.355
Aromatic hydrogen HA	0.1255	0.242

Table 1. Non-bonded energy parameters (OPLS-AA) force field for all atom types of polymers (PE, PVDF and PS) and Graphene (see Figure 1). The OPLS mixing rules have been applied such that $\boldsymbol{\sigma_{ij}} = \sqrt{\boldsymbol{\sigma_{ii}\sigma_{jj}}}$ and $\boldsymbol{\varepsilon_{ij}} = \sqrt{\boldsymbol{\varepsilon_{ii}\varepsilon_{jj}}}$. CA parameters identical for both graphene and the phenyl ring of PS.

To calculate the energetics of the polymer graphene interaction, the positional data for the polymer and graphene from the production run were separated into two additional trajectories. The energetics from these trajectories were then recalculated and compared to the original, combined, energetics. The difference in energy between the two energies (($E_{polymer\ only}$ + $E_{graphene\ only}$) - $E_{combined}$) = $E_{interaction}$ was divided across the total interaction volume of the graphene (using the cutoff of 1.1nm) to provide an interaction energy per unit volume. The size of the simulation and concentrations will likely impact the results: e.g. through the structure of graphene where multiple graphene sheets could interact, or interact via the polymer, or the (small) size of the graphene flake giving our simulations a relatively large amount of graphene edge relative to graphene surface .

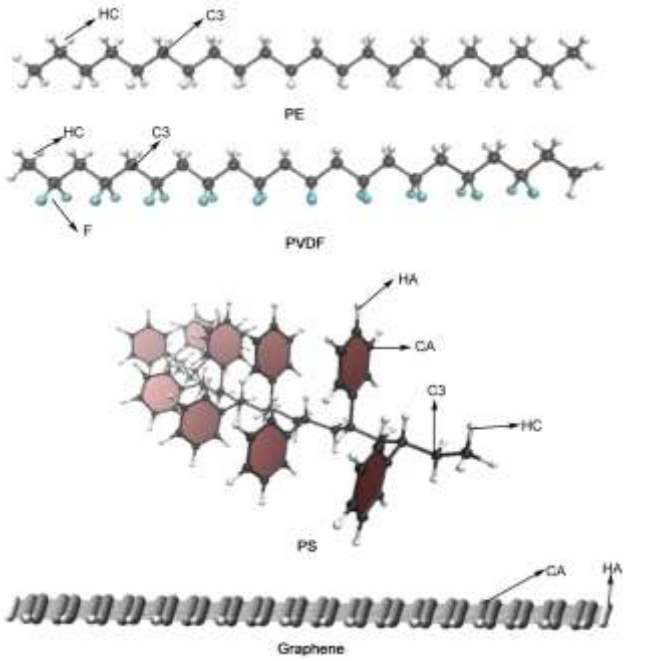

Figure 1. Structure of the studied systems indicating all atoms types.

Results and Discussion

Structure and morphology of PE, PS and PVDF

Figure 2 shows equilibrated structures for the three polymer/graphene systems at 500 K. Observing the configuration of the polymers in the three systems considered here, it can be seen that the arrangement of PE chains is well ordered and mostly parallel to the graphene surface. The well-ordered chain arrangement implies that PE has a crystalline structure. In contrast, PVDF chains display a variety of orientations that are mostly aligned perpendicular on the graphene surface. However, for PS the snapshot in Figure 2 clearly indicates an amorphous phase with randomly tangled chains.

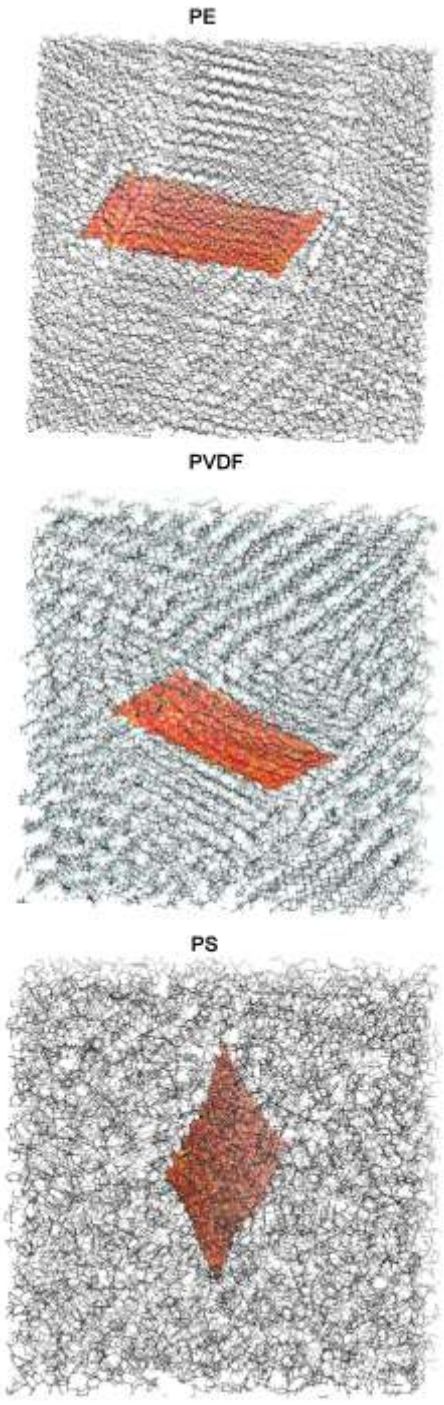

Figure 2. Cross-sectional view of the graphene-polymer nanocomposites (PE, PVDF and PS) systems after simulation.

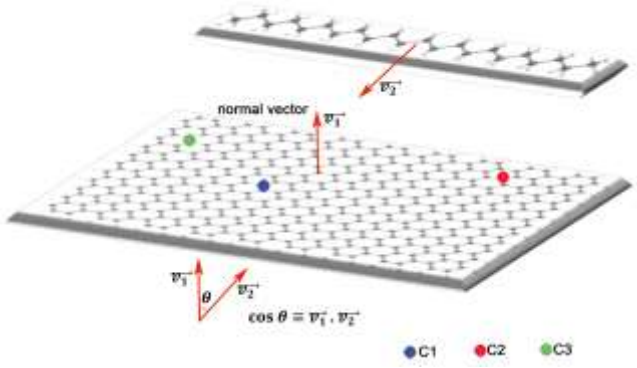

Scheme 2: Representation of two unit vectors ($\overrightarrow{v_1}$ and $\overrightarrow{v_2}$) defined for graphene and the polymer units.

A pair distribution function (PCF), $g(r\perp)$) analysis was performed using three functions $g(r)$, $g(\vartheta)$ and $g(r,\vartheta)$ in order to scrutinise the polymer conformations and structural properties. The distribution function used here is slightly different from standard RDFs, as it accounts for both distances along the normal vector from the graphene plane and angles of the backbone H/F bonds in the analysis. Our pair distribution function computes the normalized probability of finding a polymer at a given vertical distance from the graphene surface with a specific orientation of the backbone. To compute this, two vectors ($\overrightarrow{v_1}$ and $\overrightarrow{v_2}$) are defined (see Scheme 2): the first one defines the normal vector to the graphene plane and is obtained by taking three graphene atoms (denoted as C1, C2, C3) (see scheme 2 for visual representation) and defining the normal to these three atoms as $\overrightarrow{v_1}$; any three atoms are sufficient, using a different set does not significantly alter the function. Each simulation frame uses a newly defined $\overrightarrow{v_1}$ allowing graphene sheet motions to be correlated. $\overrightarrow{v_2}$ defines a vector for each of the backbone units, bisecting the H-C-H, F-C-F or H-C-phenyl angles. The angle between two unit vectors (θ) is given by the dot product $\cos\theta \equiv \overrightarrow{v_1}.\overrightarrow{v_2}$. r is the distance between the graphene and polymer units.

The pair distribution functions, computed for the three nanocomposite systems, are given in Figure 3. Colour coding is used to denote the normalized density of backbone units within each bin defined by a specific distance and angle pair. The graphene sheets have been placed in the centre of the simulation box surrounded by polymers, so the centre of each sheet is located at the origin. Negative distance values were used in the plot to denote polymers below the graphene surface whereas positive values denote polymers above the graphene.

As evident from the pair correlation function Figure 3, PE exhibits a well-ordered structure, where distinct layers are clearly visible, pointing to its fine crystalline structure. The peak for the first layer above and below the surface is considerably sharper than subsequent peaks (the innermost peaks are at ± 3.5 Å above and below the sheet), which gradually decrease in intensity. In the case of PVDF, the layering shown in the PCF is less visible in comparison to the well defined layers seen for PE, PVDF shows the presence of a few ordered layers close to the graphene surface, followed by more disordered regions. On this basis, one can describe PVDF as semi-crystalline. As seen from the PCF, PS does not display any layered structure close to the graphene surface, and overall this gives an amorphous structure. The internal self-interactions of these polymers will also play a role here and will be addressed later in detail.

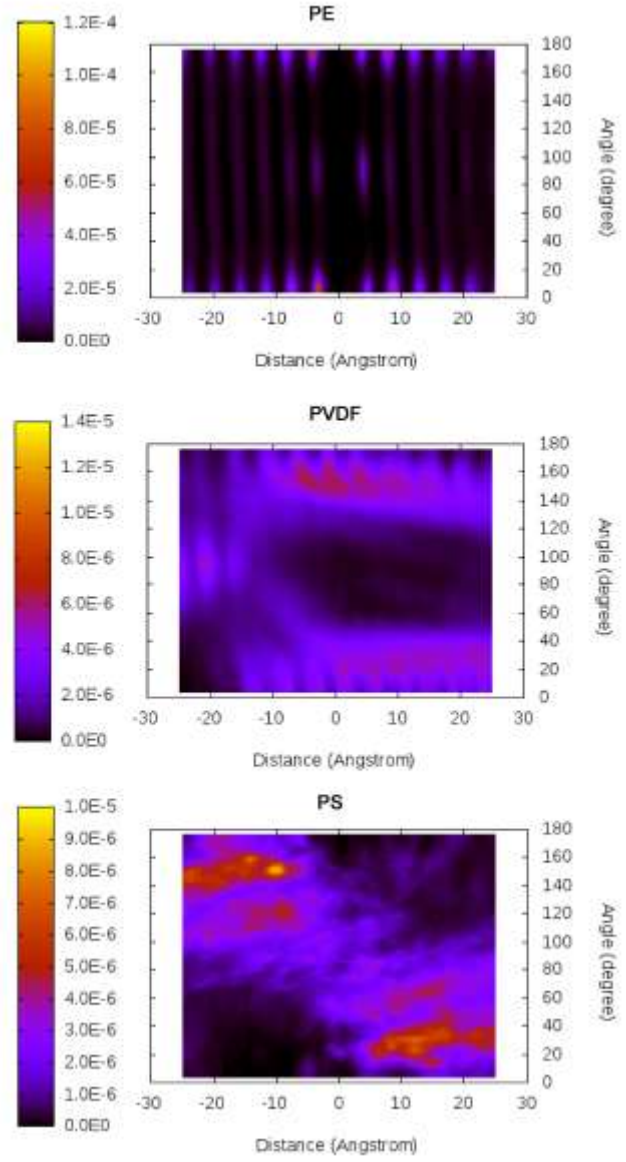

Figure 3. PCFs for PE, PVDF and PS as a function of distance and angle with respect to the graphene surface, from the simulations performed at 500 K. The colour range represents the normalized probability of finding polymer units at a given distance and angle from the graphene sheet. One should note that the magnitude of the colour scale changes with the three systems, with PS intensities an order of magnitude lower than those for PE and PVDF indicating only weakly ordered structures in PS.

The pair correlation functions are shown also in Figure 4 as a function of distance and angle separately. The distance-dependent plots, for vertical distances from the graphene sheet (Figure 4, top panel), show clearly that the layered structure is most pronounced for PE whereas PS has an evidently smeared-out distribution over distance (as expected from Figure 3). The first polymer layer with the highest population of PE forms around 3.5 Å away from graphene, in accordance with the Quantummechanical (QM) results,[22] where the shortest C (polymer) to C (graphene) distances are of the order of 3.3 to 3.4 Å. For PVDF, there is also a peak located around 10 Å (on both sides of graphene). It should, however, be emphasized that these are weak peaks and that for PVDF the polymer - polymer interaction is critical rather than the graphene - polymer one, and that in polyethylene the graphene seeds a crystal and sets the polymer orientation. To confirm the polymer end-to-end alignment a p_2(cos theta) analysis was used, which shows a strong tendency for the polymers to align along the graphene surface. Details are shown in the Appendix 2. The energetic data indicate that there is only a minimal difference between the graphene-PE and graphene-PVDF interaction strength, hence the polymer-polymer interaction must play a critical role to explain the differences between the QM and MD approaches. This is serendipitously emphasized with the formation of a small PVDF crystallite approximately 20 Å from the graphene surface. The data on the energetics are added at the end of the computational details and below in Table 2.

The reason that the orientational and positional bias observed in Figure 3 is not observable in Figure 4, is due to the sensitivity accessible by decoupling orientation and position. This point reinforces the observation that polymer-polymer interactions are critical for PDVF as already mentioned before.

In the PS case, the population is distributed almost equally over all distances, making a distinctive highest peak assessment difficult, despite the higher Tm of this material.

From analysis of the angle distribution $g(\theta)$ (Figure 4, bottom panel), it might be concluded that PVDF preferably orientates with a 30/150-degree deviation from the plane of the graphene sheet, with the maximum peak being located at around 150 degrees. In contrast, PE chains align mostly parallel to the surface of the graphene sheet (main peaks are at 0/180°). There is also a small probability for PE chains to be aligned perpendicular to the graphene plane. PS chains show no strong preference in terms of orientation angle with respect to the graphene plane, as expected in an amorphous system. The amorphous nature is likely attributable to the bulky phenyl groups and packing forces, rather than an interaction between the polymers. In view of the results, we conclude that PE prefers a closer contact with the graphene surface than PVDF and PS.

To further explore the binding preferences of the three polymers, a simple comparison of the energetics of the polymer, the graphene and the polymer with the graphene can be used (see Table 2). These show an effective binding energy between each polymer and graphene, and highlight a minimal difference in binding energy when comparing PE and PVDF, hence the critical factor must be the polymer-polymer interaction. The results emphasize that where polymer-polymer interactions are included the graphene sheet acts to disrupt the polymer-polymer interaction, hence the positive (repulsive) energy.

Please note that these results are not in contradiction with the quantummmechanically found stabilizing 1:1 interaction between graphene and the polymers as mentioned higher. The present situation indeed represents a graphene being inserted in the *bulk* polymer, implying the rupture of a lot of polymer-polymer interactions.

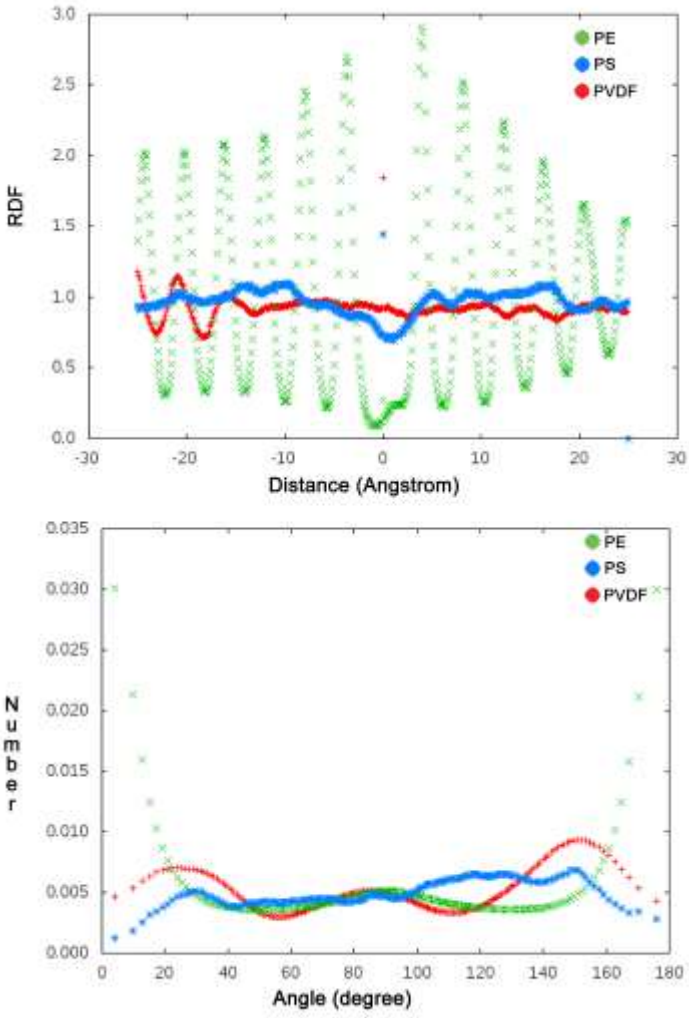

Figure 4. 2D-distribution functions for the three polymers studied, as a function of distance (top) and angle (bottom). The latter is averaged over all distances in the simulation box, up to a cut-off of 25 Angstroms.

INSERT TABLE 2!

For further analysis, we take a snapshot from each MD simulation trajectory (see Figure 5), showing (only) the position of the closest layer of a given polymer at the graphene interface. The distance refers to the gap between the first layer of the polymers and the graphene surface. In other words, it is the molecules that sit within a 3.5-7.0 Å window from the graphene. For PE and PVDF, each polymer chain is aligned mostly parallel to one another, while the distribution of the PS chains is more disordered. The PVDF polymer chains assume a well-preserved conformation, in which F atoms from one chain face H atoms in the neighbouring chain (and vice versa), providing a strong network of self-interactions.[22] The zig-zag "F-up" orientation shows by far the strongest interaction, leading to the above-mentioned organization of the second PVDF layer in which the free H atoms of the adsorbing polymer favorably interact with the F –atoms of the second polymer. Our previous non-covalent index (NCI) analysis on a pair of PVDF chains on graphene supports the presence of strong non-covalent interactions through these atoms showing more precisely a much stronger self-interaction between PVDF on graphene than between PE on graphene. As mentioned above the previous QM results[22] also showed that PVDF has the strongest interaction with the graphene, followed by PE and PS when the surface area is taken into account. However, both the MD results and the QM simulations show that the PVDF–PVDF self-interaction has a critical role in these nanocomposites. It, however, turned out that the interaction energy between PVDF and graphene is larger than the self-interaction of graphene (-13.6 vs. -12.3). Indeed Figure 3 shows PVDF polymers with F atoms pointing in one of two directions (160 degrees and 20 degrees) regardless of the side of graphene where the molecule is located. This contrasts the strong orientational preference shown by QM calculations, whereby the F atoms energetically prefer to orient up from the graphene surface. Using this metric, the QM calculations would exhibit peaks at 0 and 180 degrees for below and above the graphene sheet respectively. Figure 4 also depicts these values as a sum over all distances to highlight the lack of a strong orientational preference for PVDF.

In the case of PE we observe a strong conformational preference not shown in QM simulations. PE exhibits two favoured orientations of hydrogen atoms: in one orientation they point towards the graphene sheet whereas in the other one they point away from the graphene sheet. Both these configurations are possible with an all trans PE backbone, hence as expected both configurations are observed in equal populations (see Figure 4). PE molecules further from the graphene surface also exhibit the same orientational preference (see Figure 3), suggesting the influence of graphene extends beyond molecules in contact with the surface. These observations imply that it is the promotion of the PE crystallinity by the graphene that renders PE a good nanocomposite, rather than its strong interaction with the graphene surface.

Similarly, we note the presence of relatively strong self-interactions between PS chains in Figure 5; reducing the alignment of polymer chains on the graphene surface. This is expected from the previous computed interaction energies per surface area for this compound which was as mentioned above only 50% of the two other cases (-26.9 vs -50.4 and -50.9).
Previous NCI analysis indicates a strong CH-π type of non-covalent interactions between PS backbone and graphene is dominant. In the MD snapshot, some intermolecular π-π interactions between the aromatic rings of PS are also present, which might enhance the polymer rigidity and inflexibility resulting in a less ordered structure in comparison to PE and PVDF[22].

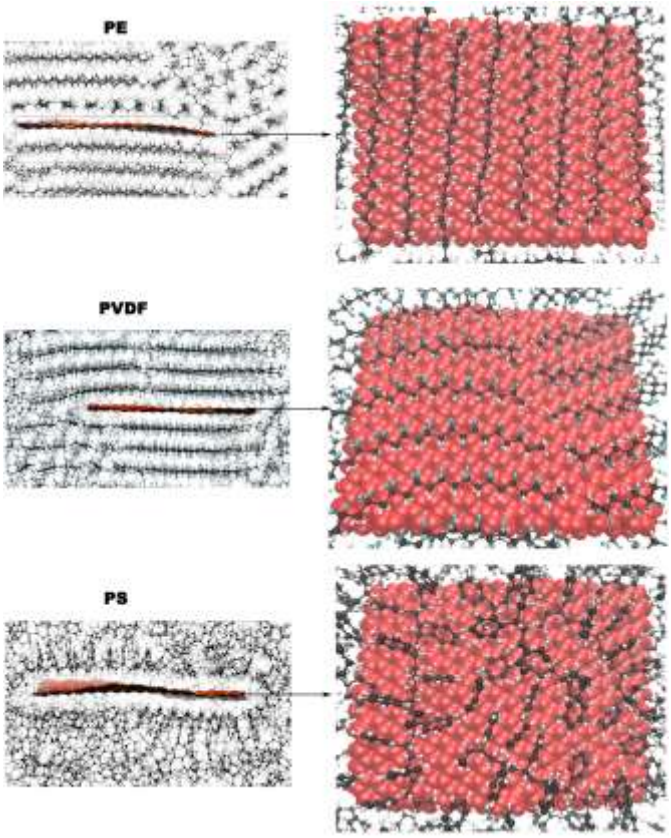

Figure 5. Representation of the first layer of polymers on the graphene surface, side view (left hand side) and top view (right hand side).

To see the direct influence of graphene in terms of nucleation and the resulting crystalline structure, we have also compared the MD simulations for the PE system after removing the graphene sheet. Figure 6 depicts two snapshots from the simulations of the two systems with and without graphene. The results show that PE is crystalline even without graphene, although now there is no preferred orientation of the PE chains. In the absence of graphene, crystallization will take place from randomly created crystal nuclei, whereas with graphene the PE chains are aligned parallel to the direction of the graphene surface (see Figure 6). This means that the first layer has an important role for determining the orientation of

the crystallisation for the remaining polymer chains, where graphene provides nucleation sites in the nanocomposite. We note that in experimental conditions, the extent of the crystallisation effect of graphene will depend on the size of the graphene sheet and the polymer chains, as well as on the synthesis conditions. Concern about the force field led us to attempt to fine tune force field parameters and test alternative force fields(GAFF). Without extensive force field improvements, the present results represent the best available option They allow us to directly compare results with carbon nanotube simulations that use the same force field. However, we note that the forcefield applied for the results presented here is flawed and leads, erroneously, to oligomers of PE crystallising at 500K. Similar findings have been published for other nanocomposites with graphene and poly (vinyl alcohol) (PVA),[33] carbon nanotubes and PE[34] and both carbon nanotubes and graphene with poly (L-lactide) (PLLA).[35] All of these studies underline the importance of the nanocarbon surface on the crystallisation of polymer chains in terms of crystal structure and morphological properties.

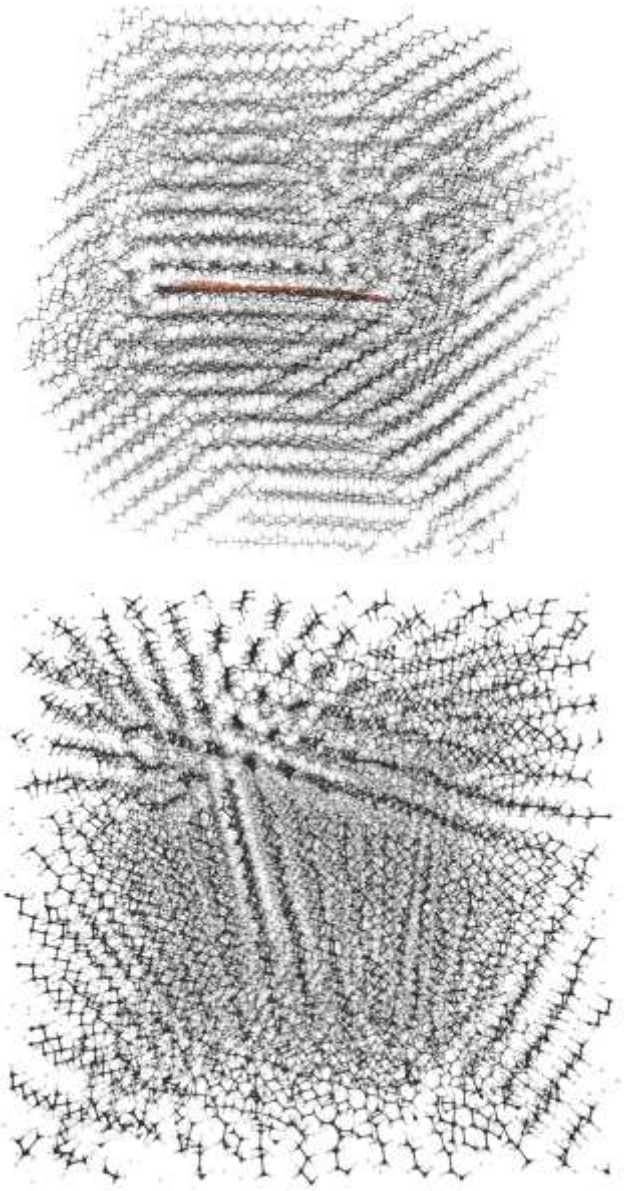

Figure 6. Two snapshots from the simulations of PE chains at 500 K with graphene (top) and without graphene (bottom).

Effect of higher temperature

Temperature has a profound effect on the crystallisation of polymers. To elaborate how nucleation and crystallisation is affected by higher temperatures, we increased the simulation temperature to 600 K (initially 500 K) for PE and PVDF, but not for PS as it is already amorphous at 500 K. The snapshots from each simulation system are compiled in Figure 7. Visual inspection of the latter suggests that PVDF has preserved its crystalline structure around the graphene sheet (in line with a higher melting point), while the PE structure is more amorphous. In particular, we observe that the outer chains in PE are more disordered than the inner ones that are still somewhat aligned on top of the graphene surface.

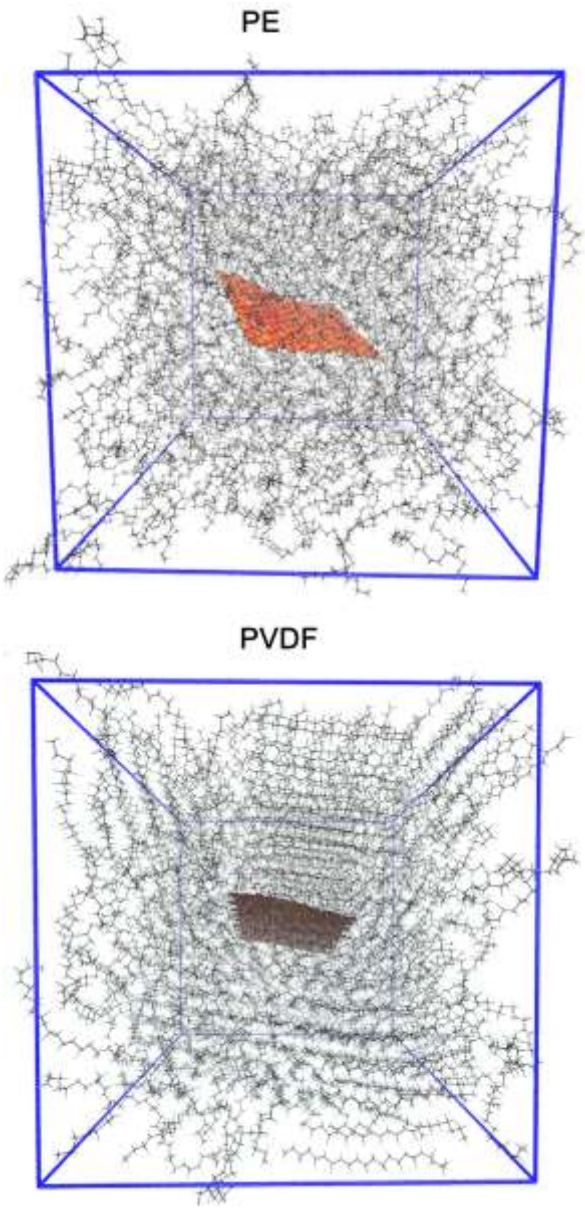

Figure 7. Cross-sectional view of the PE/graphene and, PVDF/graphene systems at an elevated temperature of 600 K. Should we add a negative comment as suggested by Martin to the caption that "minimal information can be garnered from the simulation snapshots"? or add a comment "of caution" at the end of the paragraph ?

For a direct comparison with the previous section, a PCF analysis has again been performed for these two systems at 600 K (see in Figure 8). This shows that the PE has been subject to a significant change in going from 500 K to 600 K. The uniformity of the crystalline structure has been mostly destroyed, though there is still a part that displays a weak crystallinity. For PE, the highest peak (weak in comparison to the 500 K results) is located around 3 Å, which is shifted towards shorter distances at the elevated temperature. This suggests that PE chains are moving closer to the graphene sheet, consistent with the higher mobility expected at elevated temperature.

In comparison to PE, the PVDF structure is less orientationally ordered (with respect to the Fluorine atoms). Similarly, PE is more positionally ordered than PVDF, where the RDF shows minimal PDVF order with the exception of close to the graphene sheet (see figure 8) So the nucleating effect of graphene can still be observed, but the system becomes consistently more amorphous when going further away from the graphene sheet. This is also consistent with the fact that PVDF has a higher *T*g and *T*m than PE. At 600 K, the positional order of PVDF is lost, on account of the weaker interaction with the graphene surface. However, angles between 100 and 120 degrees are weakly favoured in $g(r,\vartheta)$, indicating that there is a slight polar order arising from interchain interactions. The absence of a layered structure as observed in Figure 3 indicates an amorphous structure. For PVDF, while crystallinity is clearly lost, there is weak polar order for the fluorine atoms.

PCCP

PAPER

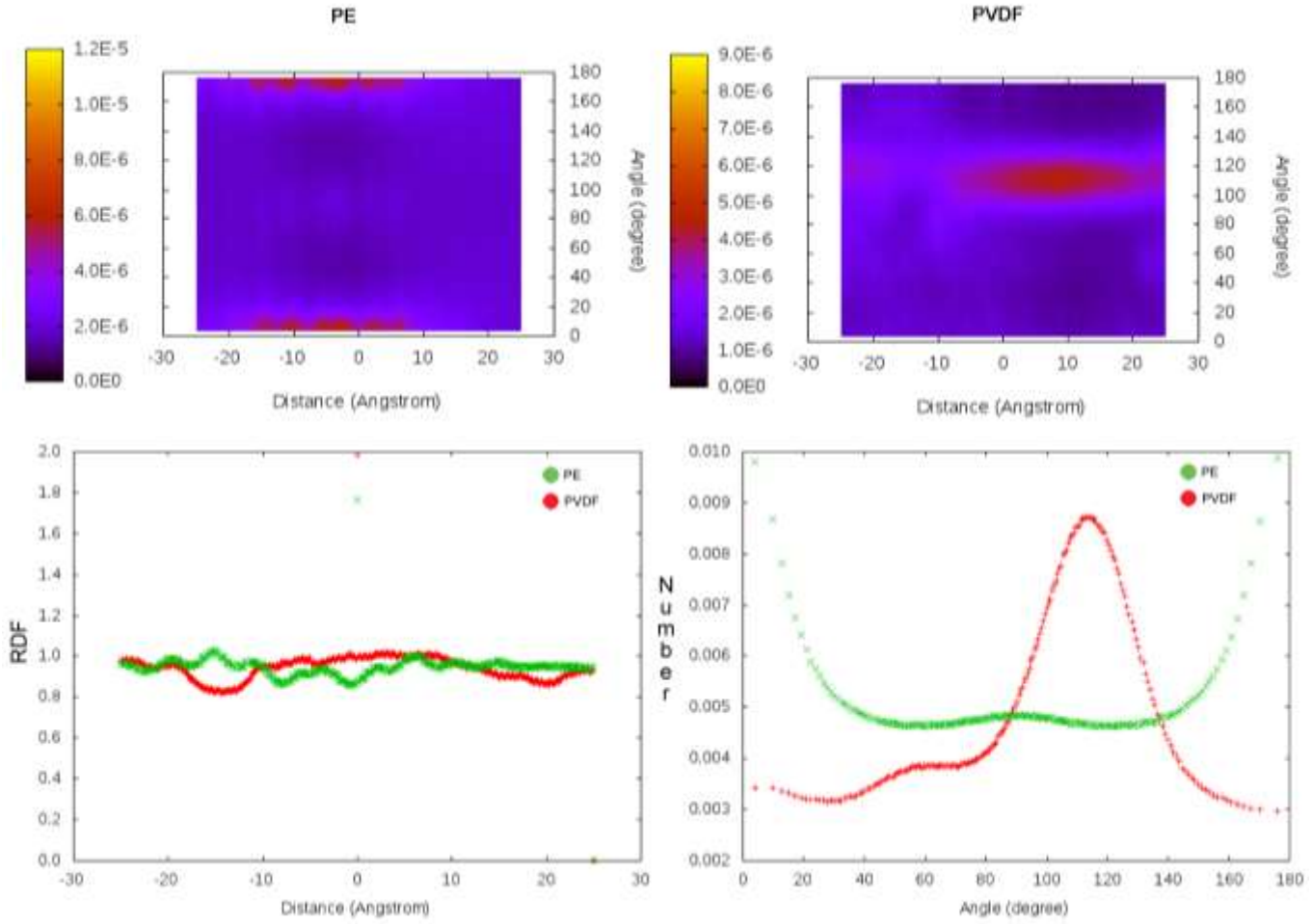

Figure 8. PCF for PE (left panel), PVDF (right panel) as a function of distance and angle from the graphene surface, from simulations performed at 600 K. The colour range represents the normalized probability of finding polymers at the given separation and angle to the surface normal. 2D plots for the two polymers depict the distributions as a function of distance (at bottom, left panel) and angle (at bottom, right panel). The colour maps have different colour scales to provide clear visibility of the topological structure and one should note that the peak heights might differ by an order of magnitude.

Conclusions

The structure and morphology of selected polymers/graphene nanocomposites have been analysed using pair correlation functions (PCF) obtained from molecular dynamics simulations. At 500 K, PE shows a higher crystallinity than PVDF whereas PS is mostly amorphous. The crystallization of PE and PVDF is influenced by the graphene plane indicating that graphene acts as a nucleation site for PE. PVDF, however, has a somewhat more complicated behavior. Small polymer crystallites form off the graphene surface and suggest that the polymer-polymer interaction is crucial. Our results imply that there is an increase in the degree of crystallinity of PE and PVDF with addition of graphene. In conclusion, graphene is a potential candidate for reinforcement of polymers.

Increasing the temperature to 600 K destroys the crystalline structure for PE. For PVDF the graphene polymer interaction is weakened by the increase in temperature, but interchain interactions remain promoting polar order.

The overall results are in line with a recent quantummechanical study by some of the present authors.[22]

Appendix 1: Equilibration Data

The two figures below show the autocorrelation functions at 500 and 600K indicating that sufficient equilibration has been performed. In addition to this, the pre-equilibration procedure is extensive. At higher temperatures, the relaxation of molecules is more rapid (see 600K autocorrelation functions).

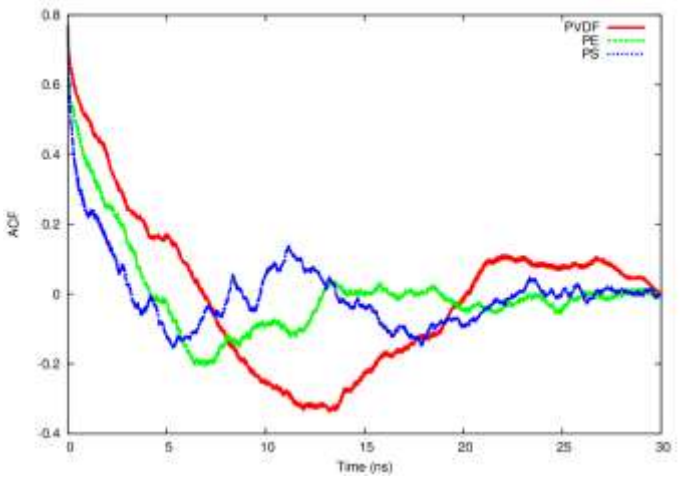

Figure A.1. Auto correlation functions of $\mathbf{P_2}\,(\boldsymbol{\cos\vartheta}) = \frac{3}{2}\boldsymbol{\cos^2\vartheta} - \frac{1}{2}$ where ϑ is the angle between the polymer end to end vector and the vector normal to the graphene for PVDF (red), PE (green) and PS (blue) at 500K. Note the rapid relaxation for PE and PS, while PVDF takes considerably longer.

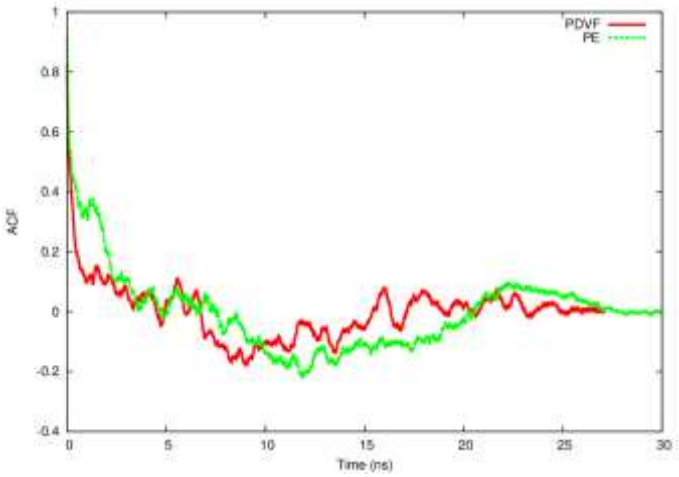

Figure A.2 Auto correlation functions of $\mathbf{P_2}\,(\boldsymbol{\cos\vartheta}) = \frac{3}{2}\boldsymbol{\cos^2\vartheta} - \frac{1}{2}$ where ϑ is the angle between the polymer end to end vector and the vector normal to the graphene for PVDF (red) and PE (green) at 600K. Note the rapid relaxation for both polymers.

Appendix 2

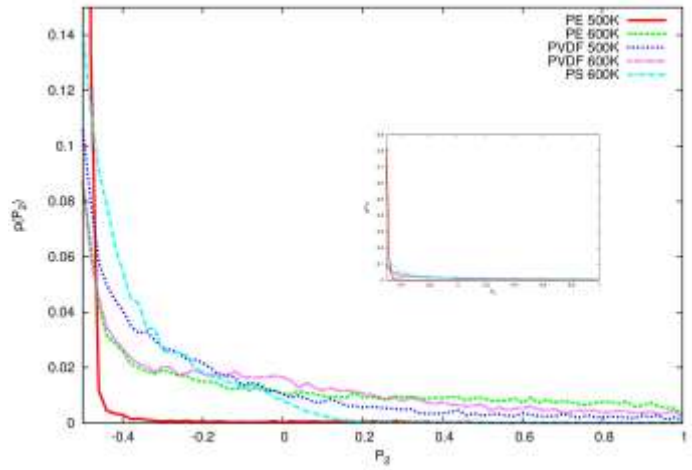

Acknowledgement

The authors would like to acknowledge the financial support of SOLVAY, S. A. In addition, the authors acknowledge support from the COST Materials, Physical and Nanosciences (MPNS) Action MP0901: ''Designing Novel Materials for Nanodevices – From Theory to Practice (NanoTP)''. Prof. Gregory Van Lier is gratefully acknowledged for interesting discussions at the VUB.

References

1 K. S. Novoselov, A. K. Geim, S. V. Morozov, D. Jiang, Y. Zhang, S. V. Dubonos, I. V. Grigorieva, A. A. Firsov, *Science,* 2004**, 306**, 666-669.

2 S. Stankovich, D. A. Dikin, G. H. Dommett, K. M. Kohlhaas, E. J. Zimney, E. A. Stach, R. D. Piner, S. T. Nguyen, R. S. Ruoff, *Nature* 2006, **442**, 282.

3 H. Kim, A. A. Abdala, C. W. Macosko, *Macromolecules* 2010, **43**, 6515-6530.

4 B. Das, K. E. Prasad, U. Ramamurty, C. N. R. Rao, *Nanotech.* 2009, **20**, 125705.

5 A. N. Rissanou, V. Harmandaris, *Soft Matter.* 2014, ***10***, 2876-2888.

6 A. Minoia, L. Chen, D. Beljonne, R. Lazzaroni, *Polym.* 2012, **53**, 5480.

7 T. Ramanathan, A.A. Abdala, S. Stankovich, D.A. Dikin, M. Herrera-Alonso, R.D. Piner, D.H. Adamson, H.C. Schniepp, X. Chen, R. S. Ruoff, S.T. Nguyen, I.A. Aksay, R.K. Prud'Homme, L.C. Brinson, *Nat.Nanotech.,* 2008, **3**, 327-331.

8 C. Lv, Q. Xue, D. Xia, M. Ma, J. Xie, H. Chen, *J. Phys. Chem. C* 2010, **114**, 6588-6594.

9 E.N. Skountzos, A. Anastassiou, V.G. Mavrantzas, D.N. Theodorou, *Macromol.,* 2014, **47**, 8072-8088.

10 P. Bacova, A.N. Rissanou, V. Harmandaris, *Macromol.,* 2015, **48,** 9024-9038.

11 H. Kawai, *Jpn. J. Appl. Phys.* 1969, 975.

12 H. Nalwa, Ferroelectric Polymers, *Marcel Dekker, NewYork* 1995, 353.

13 R. Hasegawa, Y. Takahashi, Y. Chatani, H. Tadokoro, *Polym J* 1972, **3**, 600.

14 A. Lovinger, J. *Polym.* 1981, **22**, 412.

15 S. Ramasundaram, S. Yoon, K. J. Kim, Park, C. *J. Polym. Sci. B: Polym. Phys.* 2008, **46**, 2173.

16 K. Matsushige, K. Nagata, S. Imada, T. Takemura, *Polym.* 1980, **21**, 1391.

17 D. Yang, Y. Chen, *J. Mater. Sci. Lett.* 1987, **6**, 599.

18 A. Lund, C. Gustafsson, H. Bertilsson, R. W. Rychwalski, *Compos. Sci. Tech.* 2011, **71**, 222.

19 N. A. Pertsev, A. G. Zembilgotov, *Macromol.* 1994, ***27***, 6936.

20 S. M. Hong, S. S. Hwang, *J. Nanosci. Nanotech.* 2008, **8**, 4860-4863.

21 M. A. Rahman, B. C. Lee, D.T. Phan, G. S. Chung, *Smart Mater. Struct.* 2013, **22**, 085017.

22 S. Güryel, M. Alonso, B. Hajgató, Y. Dauphin, G. Van Lier, P. Geerlings, F. De Proft, *J.Mol. Model,* 2017, **23**, 43.

23 M. Parrinello, A. Rahman, *J. Appl. Phys.* 1981, **52**, 7182-7190.

24 W. G. Hoover, *Phys. Rev. A* 1985, **31**, 1695-1697.

25 S. Nosé, *Mol. Phys.* 1984, **52**, 255-268.

26 B. Hess, C. Kutzner, D. van der Spoel, E. Lindahl, *J. Chem. Theor. Comput.* 2008, **4**, 435-447.

27 W. L. Jorgensen, D. S. Maxwell, J. Tirado-Rives, *J. Am. Chem. Soc.,* 1996, **118**, 11225-11236.

28 M. L. P. Price, D. Ostrovsky, W. L. Jorgensen, *J. Comput. Chem.* 2001, **22**, 1340-1352.

29 S.W.I. Siu, K. Pluhackova, R. A. Böckmann, *J.Chem.Theor.Comp.,* 2012, **8**, 1459-1470.

30 E.K. Watkins, W.L. Jorgensen, *J.Phys.Chem.A,* 2001, **105**, 4118-4125.

31 U. Essmann, L. Perera, M. L. Berkowitz, T. Darden, H. Lee, L. G. Pedersen, *J. Chem. Phys.* 1995, **103**, 8577-8593.

32 B. Hess H. Beckher. H.J.C. Berendsen J.G.E.M. Fraaije, *J. Comput. Chem.* 1997**, 18**, 1463**–**1472.

33 S. Lee, J. Y. Hong, J. Jang, *Polym. Int.* 2013**, 62**, 901-908.

34 R. Haggenmueller, J. E. Fischer, K. I. Winey, *Macromol.* 2006**, 39**, 2964-2971.

35 J. Z. Xu, T. Chen, C. L. Yang, Z. M. Li, Y. M. Mao, B. Q. Zeng, B. S. Hsiao, *Macromol.,* 2010**, 43**, 5000-5008.